Journal of Sound and Vibration (1990) **139**(2), 179–199

VIBRATION TRANSMISSION THROUGH ROLLING ELEMENT BEARINGS, PART I: BEARING STIFFNESS FORMULATION

T. C. LIM† AND R. SINGH

Department of Mechanical Engineering, The Ohio State University, Columbus, Ohio 43210, *U.S.A.*

(*Received* 9 *May* 1989)

Current bearing models, based on either ideal boundary condition or purely translational stiffness element description, cannot explain how the vibratory motion may be transmitted from the rotating shaft to the casing and other connecting structures in rotating mechanical equipment. For example, a vibration model of a rotating system based upon the existing bearing models can predict only the purely in-plane type motion on the flexible casing plate given only the bending motion on the shaft. However, experimental results have shown that the casing plate motion is primarily flexural or out-of-plane type. In this paper this issue is clarified quantitatively and qualitatitively by developing a new mathematical model for the precision rolling element bearings from basic principles. A comprehensive bearing stiffness matrix $[K]_{bm}$ of dimension six is proposed which clearly demonstrates a coupling betweeen the shaft bending motion and the flexural motion on the casing plate. A numerical scheme which involves a solution of non-linear algebraic equations is proposed for the estimation of the stiffness coefficients given the mean bearing load vector. A second method which requires the direct evaluation of these stiffness coefficients given the mean bearing displacement vector is also discussed. Some of the translational stiffness coefficients of the proposed bearing matrix have been verified by using available analytical and experimental data. Further validation of $[K]_{bm}$ is not possible as coupling coefficients are never measured. Also, parametric studies on the effect of unloaded contact angle, preload or bearing type are included. These results lead to a complete characterization of the bearing stiffness matrix. The theory is used to analyze vibration transmission properties in the companion paper, Part II.

1. INTRODUCTION

Current rotor dynamic models describe precision rolling element bearings either as ideal boundary conditions for the shafts [1–3], or as purely translational stiffness elements [4–6]. Such simple bearing models may be adequate for the free and forced vibration analyses of the rotor dynamic system enclosed in a rigid casing but these mathematical models cannot explain how the vibratory motion may be transmitted from the rotating shaft to the flexible or rigid casing and other connecting structures. For example, a vibration model of a system similar to Figure 1, based upon the existing bearing models, can predict only purely in-plane type motion on the flexible casing plate given only the bending motion on the shaft. However, experimental results have shown that the casing plate motion is primarily flexural or out-of-plane type [7–9]. This paradox is essentially due to an incomplete understanding of the bearing as a vibratory motion transmitter in rotating mechanical equipment including geared drives where structure-borne noise paths through bearings are often dominant.

In this paper this issue is clarified qualitatively and quantitatively by developing a new mathematical model of the precision rolling element bearings. A schematic of a generic

† Presently with Structural Dynamics Research Corporation, Milford, Ohio 45150, U.S.A.

0022-460X/90/110179+21 $03.00/0

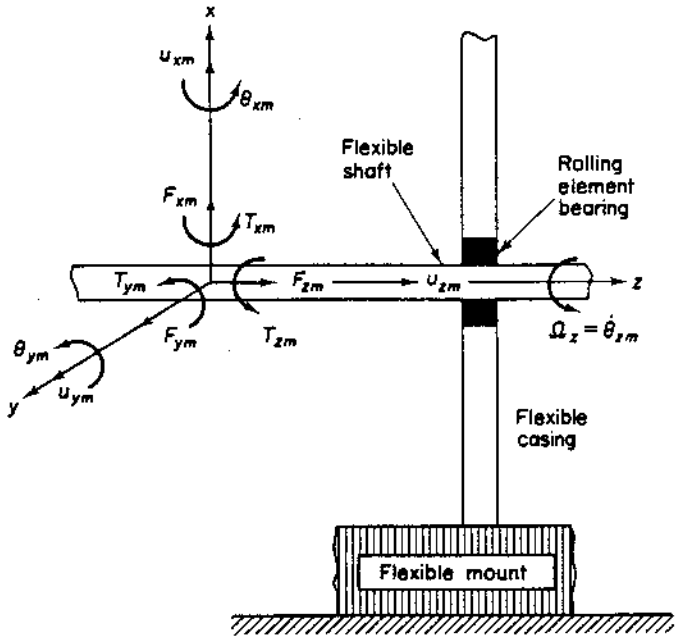

Figure 1. Schematic representation of the vibration transmission problem. Here the flexible shaft is subjected to mean forces F_{im} and torques T_{im}, where $i = x$, y or z is the direction and subscript m implies mean. Also, θ is the angular displacement and u is the translational displacement.

system with a flexible shaft rotating at speed Ω_z and subjected to a mean load vector $\{f\}_{sm} = \{F_{im}, T_{im}\}$, $i = x, y, z$, flexible casing and mount is shown in Figure 1; the shaft is supported on one of the following bearings: deep groove ball bearing, angular contact ball bearing, thrust ball bearing, straight roller bearing or taper roller bearing. A new bearing stiffness matrix $[K]_{bm}$ will be proposed which is expected to demonstrate a coupling between the shaft bending motion and the flexural motion of the casing plate. It will be shown that the translational bearing stiffness coefficients currently used in rotor dynamic models are a small subset of the proposed $[K]_{bm}$. Several example cases are employed to validate our theory. Our bearing model can be easily incorporated in analytical or numerical models typically used for the dynamic analyses—this is the basis of Part II.

2. LITERATURE REVIEW

The ideal boundary conditions for the shaft have typically been assumed to be simply supported for short bearings, clamped for long bearings or free (in the torsional mode only) [1–3]. In other cases, researchers describe the bearing as time-invariant translational springs with stiffness coefficients k_{brr} and/or k_{bzz} in the radial and axial directions, respectively [4–6, 10] (a list of symbols is given in the Appendix). Formulas for such non-linear stiffness coefficients have been given by Harris [11] and Gargiulo [5]; these are derived from the radial or axial mean force-displacement equation commonly used by precision rolling element bearing designers [11, 12]. Their derivations neglect the effects of radial clearance and mean bearing force vector $\{f\}_{bm}$ on the load distribution and hence are applicable only for a constant load angle ψ_l of 180 degrees. White refined these formulations by using a finite difference approximation for the computation of stiffness coefficients for radial ball and roller bearings, and by including the effects of radial clearance and force on the load angle ψ_l [10]. Even with these refinements the mathematical model is still inadequate and incapable of predicting the vibration transmission across bearings.

In 1982 Rajab [13] realized the limitations of the current simple theory and philosophically proposed two additional stiffness terms $k_{br\theta}$ and $k_{b\theta\theta}$ which couple the relative radial and rotational bearing displacements between the inner and outer rings, given the mean radial load and moment about the axis transverse to the radial line of action. However, our investigation, as demonstrated later in sections 4 and 5, has shown that his analyses of the ball and taper roller bearings were erroneous and resulted in an incorrect 2×2 bearing stiffness matrix. In 1988 Young [14] extended Rajab's [13] analyses to include the mean axial force F_{bzm}, and then used a discrete summation over all of the loaded rolling elements to obtain bearing forces and moment instead of the integral form while still retaining other features of Rajab's model. This resulted in a 3×3 bearing stiffness matrix which our investigation has again found to be incorrect. Some of the salient features of Rajab's [13] and Young's [14] models have been summarized in reference [15].

Experimental determination of the bearing stiffness coefficients has been strictly limited to the translational coefficients k_{brr} and k_{bzz}. A method for the measurement of *in situ* bearing stiffness under oscillating loading conditions has been given by Walford and Stone [16]. Recently, Kraus *et al.* [17] designed an *in situ* measurement test stand to determine the translational bearing stiffness from measured vibration spectra, in conjunction with the single-degree-of-freedom system theory. They determined the effect of preload, bearing release and rotational speed Ω_z on k_{brr} and k_{bzz}. Their results show that k_{brr} and k_{bzz} are essentially linear, and that the effect of Ω_z is negligible when a high preload is applied on the bearing.

3. ASSUMPTIONS AND OBJECTIVES

Due to the following key differences, a separate formulation of $[K]_{bm}$ for both ball and roller type rolling element bearings is required: (i) ball bearings have elliptical contacts and roller types have rectangular contacts between the inner race, rolling elements and outer race when loaded, and (ii) the loaded contact angles α_j of the ball types may change but α_j in the roller type remains relatively constant [18]. Each bearing is characterized by its kinematic and design parameters such as unloaded contact angle α_0, radial clearance r_L, effective stiffness coefficient K_n for inner ring-single rolling element-outer ring contacts, angular misalignment, preloads, radius of inner raceway groove curvature center for ball type and bearing pitch radius for roller type [11, 12, 18]. It is expected that $[K]_{bm}$ can be given in terms of these parameters.

The mean bearing displacements $\{q\}_{bm}$ as shown in Figure 2 are given by the relative rigid body motions between the inner and outer rings. The total bearing displacement vector is given as $\{q\}_b = \{q\}_{bm} + \{q\}_{ba}(t)$, where $\{q\}_{ba}(t)$ is the fluctuation about the mean point $\{q\}_{bm}$ during the steady state rotation. Accordingly, one must consider time varying bearing stiffness coefficients. However, in our analysis, such time varying bearing stiffness coefficients are neglected by assuming very small vibratory motions, i.e., $\{q\}_{ba} \ll \{q\}_{bm}$, and high bearing preloads. Consequently, only the mean bearing loads and displacements are included in the derivation of $[K]_{bm}$. The basic load–deflection relation for each elastic rolling element is defined by the Hertzian contact stress theory [11, 12, 19], and the load experienced by each rolling element is described by its relative location in the bearing raceway. Further, it is assumed that the angular position of each rolling element relative to one another is always maintained due to the rigid cages and pin retainers. Secondary effects such as centrifugal forces and gyroscopic moments on the bearing are ignored as these effects are evident only at extremely high rotational speeds. Tribological issues [19, 20] are beyond the scope of this study and hence in our analysis the bearings are assumed to be unlubricated.

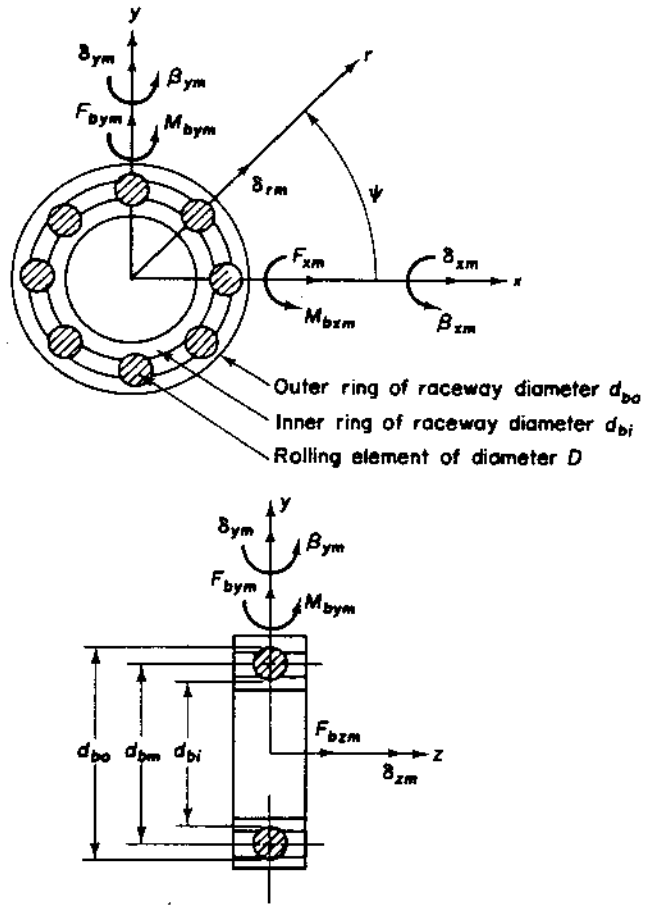

Figure 2. Rolling element bearing kinematics and co-ordinate system. Here the following nomenclature is used: d_{bo} is the outer raceway diameter, d_{bm} is the bearing pitch diameter, d_{bi} is the inner raceway diameter, ψ is the angular position of rolling element, δ_{im} is the mean translational displacement, β_{pm} is the mean angular displacement, F_{bim} is the mean bearing force, and M_{bpm} is the mean bearing moment where $i = x, y, z$ and $p = x, y$ are the directions.

The specific objectives of this study are as follows: (i) to propose and develop a new rolling element bearing stiffness matrix $[K]_{bm}$ which is suitable for the analysis of the vibration transmission through either ball or roller bearing; (ii) to develop a numerical scheme to compute $[K]_{bm}$ and discuss the existence of solutions of the non-linear algebraic bearing equations describing load–displacement relationships; (iii) to verify our proposed model by comparing its predictions with published analytical and experimental results [5, 10, 17] for the translational stiffness coefficients k_{bxx}, k_{byy} and k_{bzz}; (iv) to relate $[K]_{bm}$ to various kinematic and design parameters, and perform parametric studies to investigate the effect of unloaded contact angle α_0 and preloads; (v) to characterize the nature of $[K]_{bm}$ and recommend its usage. Finally it should be noted that dimensionless parameters will not be used here as metric units are invariably employed to specify bearings [19].

4. BEARING LOAD-DISPLACEMENT RELATIONS

In this section, the relationships between the bearing forces $\{F_{bxm}, F_{bym}, F_{bzm}\}$ and moments $\{M_{bxm}, M_{bym}\}$ transmitted through the rolling element bearing, and the bearing displacements $\{q\}_{bm}$ as given in Figure 2 will be derived for both ball and roller bearings. The mean applied loads $\{f\}_{sm}$ at the shaft as given in Figure 1 and bearing preloads generate the mean bearing displacements $\{q\}_{bm}$ and loads $\{f\}_{bm}$. These displacements $\{q\}_{bm}$ are used to derive the resultant elastic deformation $\delta(\psi_j)$ of the jth rolling element

located at angle ψ_j from the x-axis. From the ball bearing kinematics shown in Figure 3, $\delta_B(\psi_j)$ is

$$\delta_B(\psi_j) = \begin{Bmatrix} A(\psi_j) - A_0, & \delta_{Bj} > 0 \\ 0, & \delta_{Bj} \leq 0 \end{Bmatrix}, \tag{1a}$$

$$A(\psi_j) = \sqrt{(\delta^*)_{zj}^2 + (\delta^*)_{rj}^2}, \qquad (\delta^*)_{zj} = A_0 \sin \alpha_0 + (\delta)_{zj}, \qquad (\delta^*)_{rj} = A_0 \cos \alpha_0 + (\delta)_{rj}, \tag{1b-d}$$

where A_0 and A are the unloaded and loaded relative distances between the inner (a_i) and outer (a_o) raceway groove curvature centers. Similarly, for the roller bearing kinematics shown in Figure 4 for $\alpha_j = \alpha_0$, $\delta_R(\psi_j)$ is

$$\delta_R(\psi_j) = \begin{Bmatrix} (\delta)_{rj} \cos \alpha_j + (\delta)_{zj} \sin \alpha_j, & \delta_{Rj} > 0 \\ 0, & \delta_{Rj} \leq 0 \end{Bmatrix}. \tag{2}$$

Note that in equations (1) and (2) $\delta_{Bj} \leq 0$ or $\delta_{Rj} \leq 0$ implies that the jth rolling element is stress free. In both equations (1) and (2), the effective jth rolling element displacements in the axial $(\delta)_{zj}$ and radial $(\delta)_{rj}$ directions are given in Figure 5 in terms of the bearing displacements $\{q\}_{bm}$:

$$(\delta)_{zj} = \delta_z + r_j\{\beta_{xm} \sin(\psi_j) - \beta_{ym} \cos(\psi_j)\}, \qquad (\delta)_{rj} = \delta_{xm} \cos \psi_j + \delta_{ym} \sin \psi_j - r_L. \tag{3a, b}$$

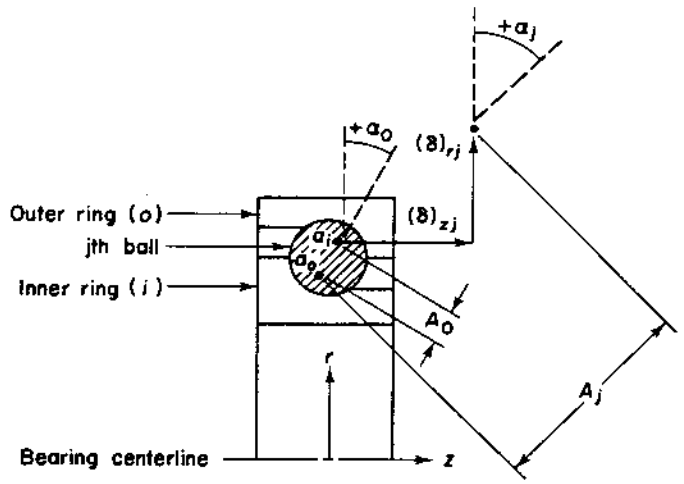

Figure 3. Elastic deformation of rolling element for non-constant contact angle α_j given by the change in the distance between the inner a_i and outer a_o raceway groove radius curvature centers due to the mean bearing loads or displacements.

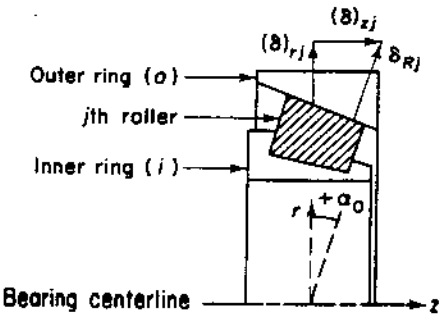

Figure 4. Elastic deformation of rolling element for constant contact angle $\alpha_j = \alpha_o$ given by the change in the relative position of the inner and outer raceways due to the mean bearing loads or displacements.

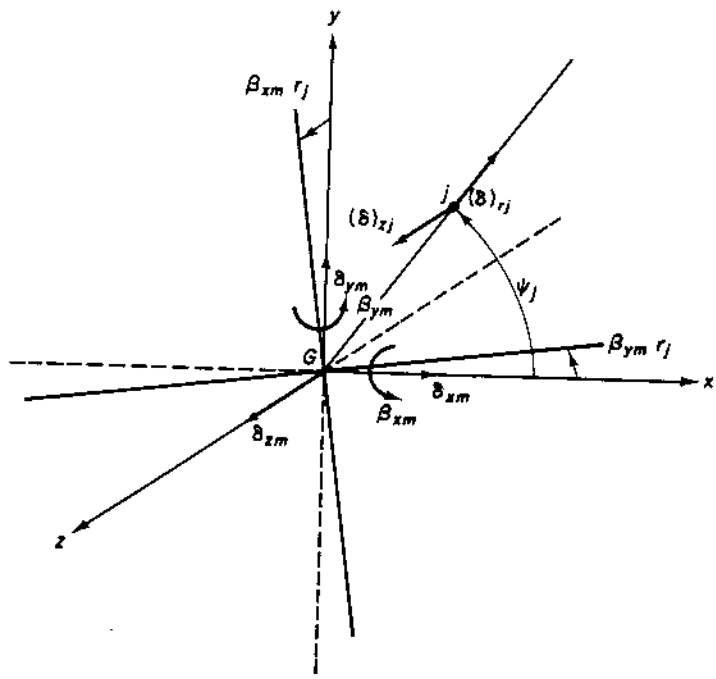

Figure 5. Decomposition of the effective radial $(\delta)_{rj}$ and axial $(\delta)_{zj}$ deformations of the jth rolling element in terms of the mean bearing displacements $\{q\}_{bm}$. Here G is the bearing outer ring geometrical center.

Here r_j is the radial distance of the inner raceway groove curvature center for the ball type or is the pitch bearing radius for roller type. Equations (1)–(3) in conjunction with the Hertzian contact stress principle [11, 12, 19] stated as follows yield the load–deflection relationships for a single rolling element:

$$Q_j = K_n \delta_j^n. \tag{4}$$

Here Q_j is the resultant normal load on the rolling element, and K_n is the effective stiffness constant for the inner race–rolling element–outer race contacts and is a function of the bearing geometry and material properties [11, 12, 18]. Note that the exponent n is equal to 3/2 for ball type with elliptical contacts and 10/9 for roller type with rectangular contacts. Previously, we have mentioned that the loaded contact angle α_j for the roller bearing remains unchanged from the unloaded position α_0, but on the other hand α_j may alter in the ball bearing case. The sign convention is such that α_j is positive when measured from the bearing x-y plane towards the axial z-axis as shown in Figures 3 and 4, and negative otherwise. For the ball bearing of Figure 3, the loaded contact angle α_j is given by

$$\tan(\alpha_j) = \{A_0 \sin\alpha_0 + (\delta)_{zj}\}/\{A_0 \cos\alpha_0 + (\delta)_{rj}\}, \tag{5}$$

where $(\delta)_{zj}$ and $(\delta)_{rj}$ are given by equations (3a) and (3b). It is appropriate here to note that Rajab [13, 15] and Young [14, 15] in their derivation of the bearing stiffness model used an expression similar to equation (2) but with $\delta_{xm} = \beta_{ym} = \delta_{zm} = r_L = 0$ in Rajab's analysis and $\delta_{xm} = \beta_{ym} = r_L = 0$ in Young's analysis for both ball and roller bearings. Since always α_j is given by equation (5) irrespective of the formulation and since equation (2) is valid only if $\alpha_j = \alpha_0$, their ball and roller bearings analyses are obviously incorrect. Expressions similar to equations (1)–(5) with minor differences have also been used by Eschmann *et al.* [18], Jones [21] and Davis [22], but their intentions were to calculate static bearing forces rather than to derive the bearing stiffness models for vibration transmission analysis.

5. DEVELOPMENT OF BEARING STIFFNESS MATRIX $[K]_{bm}$

Our proposed bearing stiffness matrix $[K]_{bm}$ is a global representation of the bearing kinematic and elastic characteristics as it combines the effects of z number of loaded rolling element stiffness in parallel by $\delta_j > 0$. First, we need to relate the resultant bearing mean load vector $\{f\}_{bm}$ to the bearing displacement vector $\{q\}_{bm}$. This can be achieved through vectorial sums $Q_j(\delta_{im}, \beta_{pm}; i = x, y, z \text{ and } p = x, y)$ in equation (4) for all of the loaded rolling elements, and this leads to the following bearing moments $\{M_{bim}\}$ and forces $\{F_{bim}\}$:

$$\begin{Bmatrix} M_{bxm} \\ M_{bym} \\ M_{bzm} \end{Bmatrix} = \sum_j^z r_j Q_j \sin\alpha_j \begin{Bmatrix} \sin\psi_j \\ -\cos\psi_j \\ 0 \end{Bmatrix}, \qquad \begin{Bmatrix} F_{bxm} \\ F_{bym} \\ F_{bzm} \end{Bmatrix} = \sum_j^z Q_j \begin{Bmatrix} \cos\alpha_j \cos\psi_j \\ \cos\alpha_j \sin\psi_j \\ \sin\alpha_j \end{Bmatrix}. \tag{6a, b}$$

Expressing Q_j and α_j in equation (6) in terms of $\{\delta_{im}, \beta_{pm}\}$ yields the following explicit relationships between $\{f\}_{bm}$ and $\{q\}_{bm}$ for ball bearings:

$$\begin{Bmatrix} M_{bxm} \\ M_{bym} \\ M_{bzm} \end{Bmatrix} = K_n \sum_j^z \frac{\{\sqrt{[A_0 \sin\alpha_0 + (\delta)_{zj}]^2 + [A_0 \cos\alpha_0 + (\delta)_{rj}]^2} - A_0\}^n}{\sqrt{[A_0 \sin\alpha_0 + (\delta)_{zj}]^2 + [A_0 \cos\alpha_0 + (\delta)_{rj}]^2}} \times r_j \{A_0 \sin\alpha_0 + (\delta)_{zj}\} \begin{Bmatrix} \sin\psi_j \\ -\cos\psi_j \\ 0 \end{Bmatrix}, \tag{7a}$$

$$\begin{Bmatrix} F_{bxm} \\ F_{bym} \\ F_{bzm} \end{Bmatrix} = K_n \sum_j^z \frac{\{\sqrt{[A_0 \sin\alpha_0 + (\delta)_{zj}]^2 + [A_0 \cos\alpha_0 + (\delta)_{rj}]^2} - A_0\}^n}{\sqrt{[A_0 \sin\alpha_0 + (\delta)_{zj}]^2 + [A_0 \cos\alpha_0 + (\delta)_{rj}]^2}} \times \begin{Bmatrix} [A_0 \cos\alpha_0 + (\delta)_{rj}] \cos\psi_j \\ [A_0 \cos\alpha_0 + (\delta)_{rj}] \sin\psi_j \\ [A_0 \sin\alpha_0 + (\delta)_{zj}] \end{Bmatrix}. \tag{7b}$$

Similarly, for roller bearings, one obtains

$$\begin{Bmatrix} M_{bxm} \\ M_{bym} \\ M_{bzm} \end{Bmatrix} = K_n \sin\alpha_0 \sum_j^z r_j \{(\delta)_{rj} \cos\alpha_0 + (\delta)_{zj} \sin\alpha_0\}^n \begin{Bmatrix} \sin\psi_j \\ -\cos\psi_j \\ 0 \end{Bmatrix}, \tag{8a}$$

$$\begin{Bmatrix} F_{bxm} \\ F_{bym} \\ F_{bzm} \end{Bmatrix} = K_n \sum_j^z \{(\delta)_{rj} \cos\alpha_0 + (\delta)_{zj} \sin\alpha_0\}^n \begin{Bmatrix} \cos\alpha_0 \cos\psi_j \\ \cos\alpha_0 \sin\psi_j \\ \sin\alpha_0 \end{Bmatrix}. \tag{8b}$$

Here $(\delta)_{rj}$ and $(\delta)_{zj}$ are functions of $\{\delta_{im}, \beta_{pm}\}$ as defined by equation (3). Approximate integral forms of equations (7a, b) and (8a, b) are often used instead of the summation forms to eliminate explicit dependence on ψ_j, especially in the case of only one or two degrees of freedom bearings [11, 19]. For instance, Rajab [13, 15] chose the integral form representation, but made a mathematical error in constructing the integrand which led to further errors in his analysis.

Now we define a symmetric bearing stiffness matrix $[K]_{bm}$ of dimension six from equations (7a, b) and (8a, b) and by assuming that $\{q\}_{ba} \ll \{q\}_{bm}$:

$$[K]_{bm} = \begin{bmatrix} \partial F_{bim}/\partial\delta_{jm} & \partial F_{bim}/\partial\beta_{jm} \\ \partial M_{bim}/\partial\delta_{jm} & \partial M_{bim}/\partial\beta_{jm} \end{bmatrix}_{\{q\}_{bm}}, \qquad i, j = x, y, z. \tag{9}$$

Here each stiffness coefficient must be evaluated at the mean point $\{q\}_{bm}$. Explicit expressions for the ball bearing stiffness are as follows (note that $[K]_{bm}$ is symmetric, i.e., $k_{bij} = k_{bji}$):

$$k_{bxx} = K_n \sum_j^z \frac{(A_j - A_0)^n \cos^2 \psi_j \left\{ \frac{nA_j(\delta^*)_{rj}^2}{A_j - A_0} + A_j^2 - (\delta^*)_{rj}^2 \right\}}{A_j^3}, \tag{10a}$$

$$k_{bxy} = K_n \sum_j^z \frac{(A_j - A_0)^n \sin \psi_j \cos \psi_j \left\{ \frac{nA_j(\delta^*)_{rj}^2}{A_j - A_0} + A_j^2 - (\delta^*)_{rj}^2 \right\}}{A_j^3}, \tag{10b}$$

$$k_{bxz} = K_n \sum_j^z \frac{(A_j - A_0)^n (\delta^*)_{rj} (\delta^*)_{zj} \cos \psi_j \left\{ \frac{nA_j}{A_j - A_0} - 1 \right\}}{A_j^3}, \tag{10c}$$

$$k_{bx\theta_x} = K_n \sum_j^z \frac{r_j (A_j - A_0)^n (\delta^*)_{rj} (\delta^*)_{zj} \sin \psi_j \cos \psi_j \left\{ \frac{nA_j}{A_j - A_0} - 1 \right\}}{A_j^3}, \tag{10d}$$

$$k_{bx\theta_y} = K_n \sum_j^z \frac{r_j (A_j - A_0)^n (\delta^*)_{rj} (\delta^*)_{zj} \cos^2 \psi_j \left\{ 1 - \frac{nA_j}{A_j - A_0} \right\}}{A_j^3}, \tag{10e}$$

$$k_{byy} = K_n \sum_j^z \frac{(A_j - A_0)^n \sin^2 \psi_j \left\{ \frac{nA_j(\delta^*)_{rj}^2}{A_j - A_0} + A_j^2 - (\delta^*)_{rj}^2 \right\}}{A_j^3}, \tag{10f}$$

$$k_{byz} = K_n \sum_j^z \frac{(A_j - A_0)^n (\delta^*)_{rj} (\delta^*)_{zj} \sin \psi_j \left\{ \frac{nA_j}{A_j - A_0} - 1 \right\}}{A_j^3}, \tag{10g}$$

$$k_{by\theta_x} = K_n \sum_j^z \frac{r_j (A_j - A_0)^n (\delta^*)_{rj} (\delta^*)_{zj} \sin^2 \psi_j \left\{ \frac{nA_j}{A_j - A_0} - 1 \right\}}{A_j^3}, \tag{10h}$$

$$k_{by\theta_y} = K_n \sum_j^z \frac{r_j (A_j - A_0)^n (\delta^*)_{rj} (\delta^*)_{zj} \sin \psi_j \cos \psi_j \left\{ 1 - \frac{nA_j}{A_j - A_0} \right\}}{A_j^3}, \tag{10i}$$

$$k_{bzz} = K_n \sum_j^z \frac{(A_j - A_0)^n \left\{ \frac{nA_j(\delta^*)_{zj}^2}{A_j - A_0} + A_j^2 - (\delta^*)_{zj}^2 \right\}}{A_j^3}, \tag{10j}$$

$$k_{bz\theta_x} = K_n \sum_j^z \frac{r_j (A_j - A_0)^n \sin \psi_j \left\{ \frac{nA_j(\delta^*)_{zj}^2}{A_j - A_0} + A_j^2 - (\delta^*)_{zj}^2 \right\}}{A_j^3}, \tag{10k}$$

$$k_{bz\theta_y} = K_n \sum_j^z \frac{r_j (A_j - A_0)^n \cos \psi_j \left\{ (\delta^*)_{zj}^2 - \frac{nA_j(\delta^*)_{zj}^2}{A_j - A_0} - A_j^2 \right\}}{A_j^3}, \tag{10l}$$

$$k_{b\theta_x\theta_x} = K_n \sum_j^z \frac{r_j^2(A_j - A_0)^n \sin^2 \psi_j \left\{ \frac{nA_j(\delta^*)_{zj}^2}{A_j - A_0} + A_j^2 - (\delta^*)_{zj}^2 \right\}}{A_j^3}, \tag{10m}$$

$$k_{b\theta_x\theta_y} = K_n \sum_j^z \frac{r_j^2(A_j - A_0)^n \sin \psi_j \cos \psi_j \left\{ (\delta^*)_{zj}^2 - \frac{nA_j(\delta^*)_{zj}^2}{A_j - A_0} - A_j^2 \right\}}{A_j^3}, \tag{10n}$$

$$k_{b\theta_y\theta_y} = K_n \sum_j^z \frac{r_j^2(A_j - A_0)^n \cos^2 \psi_j \left\{ \frac{nA_j(\delta^*)_{zj}^2}{A_j - A_0} + A_j^2 - (\delta^*)_{zj}^2 \right\}}{A_j^3}, \tag{10o}$$

$$k_{bi\theta_z} = k_{b\theta_i\theta_z} = 0, \quad i = x, y, z. \tag{10p}$$

Here $(\delta^*)_{zj}$, $(\delta^*)_{rj}$ and A_j are defined by equation (1). The roller bearing stiffness coefficients $k_{bij} = k_{bji}$ are given explicitly as

$$k_{bxx} = nK_n \cos^2 \alpha_0 \sum_j^z \delta_{Rj}^{n-1} \cos^2 \psi_j, \qquad k_{bxy} = \frac{n}{2} K_n \cos^2 \alpha_0 \sum_j^z \delta_{Rj}^{n-1} \sin 2\psi_j, \tag{11a, b}$$

$$k_{bxz} = \frac{n}{2} K_n \sin 2\alpha_0 \sum_j^z \delta_{Rj}^{n-1} \cos \psi_j, \qquad k_{bx\theta_x} = \frac{n}{4} K_n \sin 2\alpha_0 \sum_j^z r_j \delta_{Rj}^{n-1} \sin 2\psi_j, \tag{11c, d}$$

$$k_{bx\theta_y} = -\frac{n}{2} K_n \sin 2\alpha_0 \sum_j^z r_j \delta_{Rj}^{n-1} \cos^2 \psi_j, \qquad k_{byy} = nK_n \cos^2 \alpha_0 \sum_j^z \delta_{Rj}^{n-1} \sin^2 \psi_j, \tag{11e, f}$$

$$k_{byz} = \frac{n}{2} K_n \sin 2\alpha_0 \sum_j^z \delta_{Rj}^{n-1} \sin \psi_j, \qquad k_{by\theta_x} = \frac{n}{2} K_n \sin 2\alpha_0 \sum_j^z r_j \delta_{Rj}^{n-1} \sin^2 \psi_j, \tag{11g, h}$$

$$k_{by\theta_y} = -\frac{n}{4} K_n \sin 2\alpha_0 \sum_j^z r_j \delta_{Rj}^{n-1} \sin 2\psi_j, \qquad k_{bzz} = nK_n \sin^2 \alpha_0 \sum_j^z \delta_{Rj}^{n-1}, \tag{11i, j}$$

$$k_{bz\theta_x} = nK_n \sin^2 \alpha_0 \sum_j^z r_j \delta_{Rj}^{n-1} \sin \psi_j, \qquad k_{bz\theta_y} = -nK_n \sin^2 \alpha_0 \sum_j^z r_j \delta_{Rj}^{n-1} \cos \psi_j, \tag{11k, l}$$

$$k_{b\theta_x\theta_x} = nK_n \sin^2 \alpha_0 \sum_j^z r_j^2 \delta_{Rj}^{n-1} \sin^2 \psi_j, \qquad k_{b\theta_x\theta_y} = -\frac{n}{2} K_n \sin^2 \alpha_0 \sum_j^z r_j^2 \delta_{Rj}^{n-1} \sin 2\psi_j, \tag{11m, n}$$

$$k_{b\theta_y\theta_y} = nK_n \sin^2 \alpha_0 \sum_j^z r_j^2 \delta_{Rj}^{n-1} \cos^2 \psi_j, \qquad k_{bi\theta_z} = k_{b\theta_i\theta_z} = 0, \qquad i = x, y, z. \tag{11o, p}$$

Here δ_{Rj} is defined in equation (2). It should be noted that all stiffness terms associated with the torsional degree of freedom β_{zm} are zero due to the fact that an ideal bearing allows free rotation about the z-direction. Also, the translational stiffness coefficients k_{bii}, $i = x, y, z$ for $\delta_{ym} = \delta_{zm} = \beta_{xm} = \beta_{ym} = 0$, $\delta_{xm} = \delta_{zm} = \beta_{xm} = \beta_{ym} = 0$ or $\delta_{xm} = \delta_{ym} = \beta_{xm} = \beta_{ym} = 0$ are equivalent to the bearing stiffness coefficients commonly used by investigators [5, 6, 10]. The nature of these and other features of $[K]_{bm}$ will be discussed later in section 9.

6. NUMERICAL ESTIMATION OF $[K]_{bm}$

The coefficients k_{bij} can be computed by one of the following two methods: I, directly compute k_{bij} given the mean bearing displacement vector $\{q\}_{bm}$ by employing equations (10a–p) and (11a–p); II, numerically solve the non-linear algebraic equations described

by equations (7a, b) and (8a, b) to obtain $\{q\}_{bm}$ from $\{f\}_{bm}$, and then evaluate k_{bij} per method I. Note that $\{f\}_{bm}$ may be functions of the mean shaft loads, bearing preloads and shaft and casing compliances, depending on the configuration and flexibility of the rotating mechanical system. If the bearing system is statistically determinate, then $\{f\}_{bm}$ may be computed explicitly in terms of $\{f\}_{sm}$ and preloads based upon the force and moment equilibrium equations. Conversely, for an indeterminate system appropriate field equations for the shaft and casing plate are needed in addition to the equilibrium equations to obtain $\{f\}_{bm}$ which must also include shaft and casing compliances. Calculations of $\{f\}_{bm}$ and $\{q\}_{bm}$ in this case are simultaneous, which may be extensive especially when the system is very flexible, and may even require discretization by using finite element or lumped mass techniques. However, in many real machines the in-plane stiffness of the casing plate which supports most of the mean bearing load is much higher than the bending stiffness of the shaft. Hence the casing in-plane stiffness term may be neglected without contributing any error to $\{f\}_{bm}$ [11, 18]. Also only Euler's beam equation for a statically indeterminate shaft is used along with the non-linear bearing load-displacement equations (7a, b) and (8a, b).

Method I is computationally direct and needs no discussion, but method II deals with as many as 10 N non-linear algebraic equations for N bearings if the casing flexibility is neglected. One must choose an appropriate numerical method as non-linear algebraic equations must be solved iteratively [23, 24]. In addition, the available numerical methods need *a priori* knowledge of the approximate location of the solution vector being sought and hence one must be careful in interpreting the numerical results. In this paper, we adopted the Newton-Raphson method for its good convergence characteristic [23, 24]. To implement this method, equation (6) for each bearing is rearranged as

$$\begin{Bmatrix} H_1 \\ H_2 \end{Bmatrix} = \begin{Bmatrix} M_{bxm} \\ M_{bym} \end{Bmatrix} - \sum_j^z r_j Q_j \sin \alpha_j \begin{Bmatrix} \sin \psi_j \\ -\cos \psi_j \end{Bmatrix} = \begin{Bmatrix} 0 \\ 0 \end{Bmatrix}, \tag{12a}$$

$$\begin{Bmatrix} H_3 \\ H_4 \\ H_5 \end{Bmatrix} = \begin{Bmatrix} F_{bxm} \\ F_{bym} \\ F_{bzm} \end{Bmatrix} - \sum_j^z Q_j \begin{Bmatrix} \cos \alpha_j \cos \psi_j \\ \cos \alpha_j \sin \psi_j \\ \sin \alpha_j \end{Bmatrix} = \begin{Bmatrix} 0 \\ 0 \\ 0 \end{Bmatrix}, \tag{12b}$$

where $H_1, H_2, \ldots, H_5$ are functions defined for computational reasons. For an indeterminate system, there are additional functions $H_6, H_7, \ldots, H_V$ from the field equations. By using Taylor's series, any function H_k in equations (12a, b) can be expanded about the solution vector $X = \{q\}_{bm}$ for a statically determinate system and $X = [\{q\}_{bm}^T, \{f\}_{bm}^T]^T$ for a statically indeterminate system as follows by neglecting second and higher order terms:

$$H_k(X + \delta X) \approx H_k(X) + \sum_j^V \frac{\partial H_k}{\partial X_j} \delta X_j, \qquad k = 1, 2, 3, \ldots, V. \tag{13}$$

The solution for the incremental vector δX can be obtained by setting $H_k(X + \delta X) = 0$ per equations (12) and (13) which yields a set of linear algebraic equations. This vector δX is added to the previously computed vector X given by $H_k(X) = 0$ for the next iteration until the convergence criterion, say that δX is within a specified tolerance, is satisfied. Our proposed numerical scheme can be summarized as follows: (i) guess the bearing displacement vector $\{q\}_{bm}$ and/or load vector $\{f\}_{bm}$; (ii) compute δX and check against a specified tolerance; (iii) add δX to the previous solution vector X and repeat steps (i) and (ii) until the convergence criterion is satisfied. We have found that a few initial guess trials are required in most cases to obtain reasonable results.

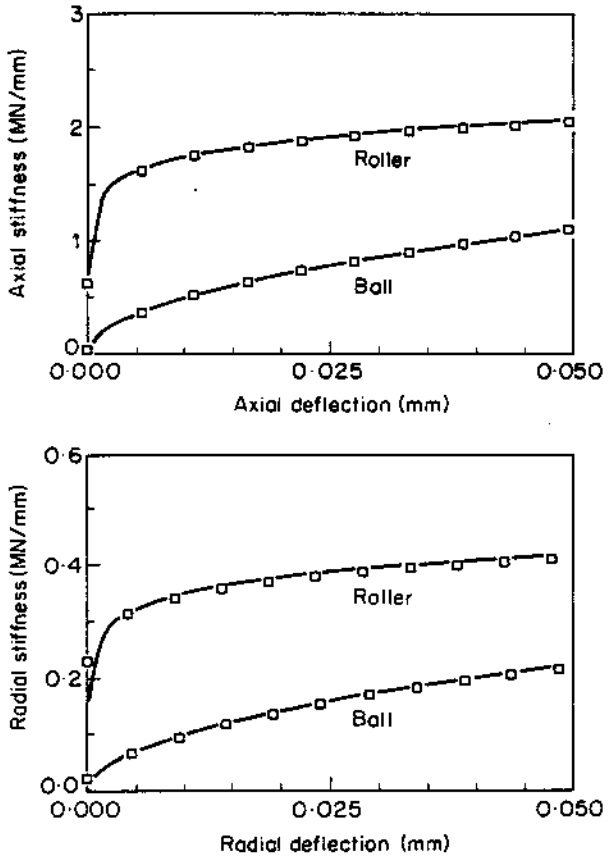

Figure 6. Comparison between the proposed theory (——) and Gargiulo's formulas [5] (□) for axial k_{bzz} and radial k_{brr} stiffness coefficients of ball and roller bearings.

7. VALIDATION OF PROPOSED MODEL

In order to validate our theory we compare the translational stiffness coefficients of the proposed bearing matrix $[K]_{bm}$ with published analytical and experimental results [5, 10, 17]. First we have applied our theory to predict the non-linear axial $k_{bzz} = k_{bzz}(\delta_{zm})$ and radial $k_{brr} = k_{brr}(\delta_{rm})$ stiffnesses as shown in Figure 6. Our predictions are found to be within 2 per cent of Gargiulo's [5] formulas which are commonly used for both ball and roller bearings.

For the second example case, we consider the ball bearings used by Kraus *et al.* [17] for an *in situ* determination of the bearing stiffness. Using their bearing design parameters, we have computed the radial stiffness coefficient k_{brr} as a function of the mean axial preload F_{bzm}. Excellent comparison between theory and experiment is seen in Figure 7.

Finally, we compare our results for the nonlinear radial stiffness k_{brr} with those reported earlier by White [10] for both ball and roller bearings. We note discrepancies in Figure 8 between our theory and White's results. In order to explain these we now define $\hat{k}_{brr}$ using the finite difference approximation which was also used by White: $\hat{k}_{brr} \approx \Delta F_{brm}/\Delta\delta_{rm} \approx F_{brm}/(\delta_{rm} - r_L)$. Now a good match is evident in Figure 8 between our $\hat{k}_{brr}$ values and the data given by White. However, the correct formulation is obviously given by our proposed theory which is based on the analytical partial derivatives $k_{brr} = \partial F_{brm}/\partial\delta_{rm}$ as the displacement δ_{rm} may be large.

8. PARAMETRIC STUDIES

The proposed matrix $[K]_{bm}$ includes a coupling between the casing flexural motion and shaft bending motion which is reflected by some of the dominant off-diagonal, $k_{bx\theta_y}$,

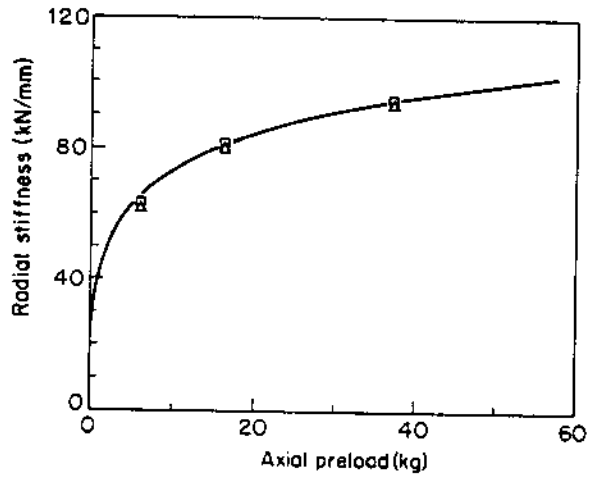

Figure 7. Comparison between the proposed theory (——) and the experimental results of Kraus *et al.* [17] for k_{brr} as a function of the mean axial preload. □, Experiment 0 rpm; △, experiment 1000 rpm.

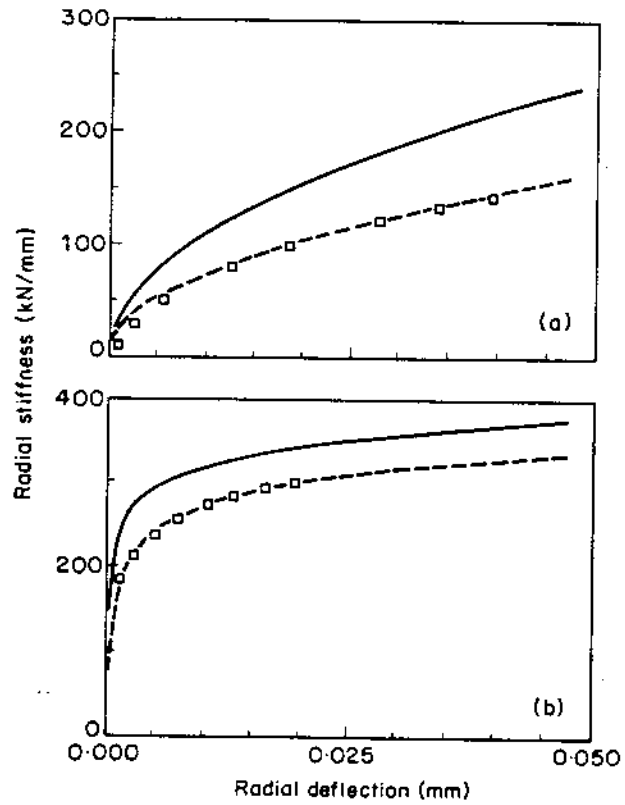

Figure 8. Comparison between the proposed theory k_{brr} (——), estimated $\hat{k}_{brr}$ (- - -), and White's analytical results [10] (□). (a) Ball bearing; (b) roller bearing.

$k_{by\theta_x}$, $k_{bz\theta_x}$ and $k_{bz\theta_y}$, and rotational diagonal, $k_{b\theta_x\theta_x}$ and $k_{b\theta_y\theta_y}$, stiffness coefficients; these are labeled as "coupling coefficients" for discussion purposes. Such stiffness coefficients are investigated further by varying preloading conditions and unloaded contact angle α_0 for both ball (set A) and roller (set B) bearings, the design data for which are listed in Table 1.

The coupling coefficients given a constant mean radial displacement δ_{rm} (radial preload), as shown in Figures 9 and 10 for both ball and roller bearings respectively, are found to increase as α_0 increases and reach a maximum when α_0 is near 90°. On the other hand, the radial translational stiffness coefficients in the x and y directions are

TABLE 1

Design parameters for typical ball and roller bearings used for parametric studies

Parameters	Set A (ball type)	Set B (roller type)
Load-deflection exponent, n	3/2	10/9
Load-deflection constant, K_n (N/m^n)	$8{\cdot}5\times10^9$	$3{\cdot}0\times10^8$
Number of rolling elements, Z	12	14
Radial clearance, r_L (mm)	0·00005	0·00175
Pitch radius, r_j (mm)‡	19·65	21·25
A_0 (mm)†	0·05	—

† Unloaded distance between inner and outer raceway groove curvature centers (see Figure 3).
‡ Radius of inner raceway groove curvature center for ball bearings given in equation (3).

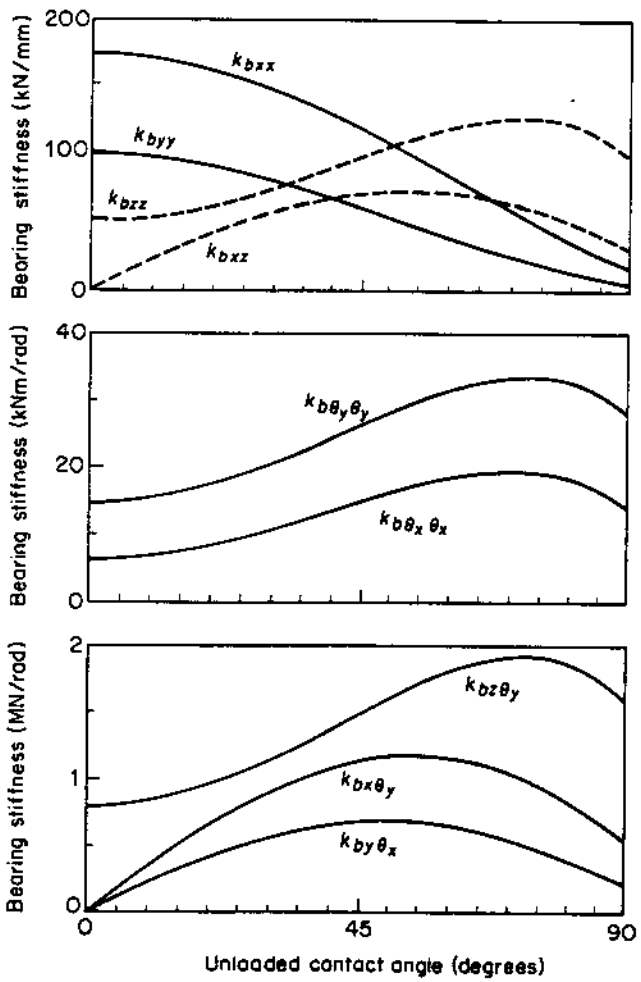

Figure 9. Dominant stiffness coefficients of ball bearing set A for $0° \leq \alpha_0 \leq 90°$ and given a constant mean radial bearing displacement $\delta_{xm} = 0{\cdot}025$ mm.

found to decrease as α_0 increases. These observations imply that for deep groove ball type or straight roller type bearing ($\alpha_0 \approx 0°$) the radial stiffness coefficients k_{brr} are dominant, but for angular contact ball type or taper roller type bearing ($\alpha_0 > 0°$) the coupling terms are more significant. Note that in Figure 10, all the stiffness coefficients are zero at $\alpha_0 = 90°$ for the roller type. This is due to the fact that in the thrust roller bearing, radial flanges are included to resist the roller motion in this direction which is not modeled here, and hence these stiffness coefficients must vanish. In addition, thrust

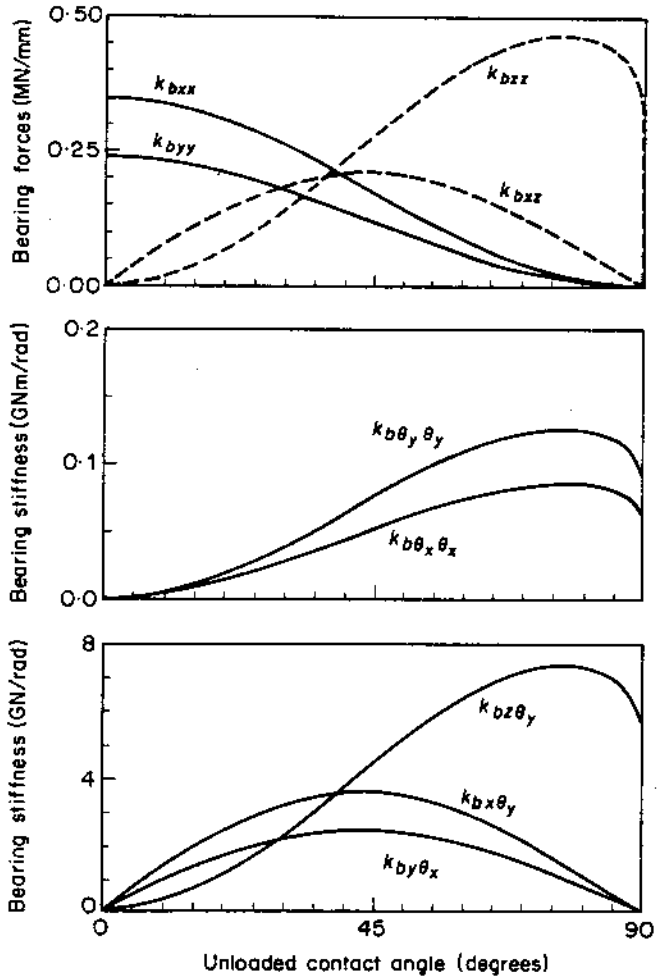

Figure 10. Dominant stiffness coefficients of roller bearing set B for $0° \leq \alpha_0 \leq 90°$ and given a constant mean radial bearing displacement $\delta_{xm} = 0{\cdot}025$ mm.

roller bearings are designed to carry axial loads [11, 18]. On the other hand, ball bearings have finite stiffness coefficients at $\alpha_0 = 90°$ due to the curvature of the raceway which provide some resistance to the radial preloads. In general, the trends in both ball and roller bearing stiffness properties are similar when each is subjected to mean radial displacement or preload.

In the case when the bearings are subjected to mean axial displacement (axial preload), as shown in Figure 11 for the ball type and Figure 12 for the roller type, the number of non-zero stiffness coefficients is less than those seen for the radial preload only. Again, it is observed that both ball and roller bearings display similar trends. Over mid to high α_0 values, the coupling coefficients are found to be significant. The translational stiffness coefficients are relatively constant except for the axial stiffness which increases as α_0 increases. This is expected due to the inclination of the rolling element line of contact from the x-y plane which increases elastic support in the z-direction. At $\alpha_0 = 0°$, all the stiffness coefficients for roller bearings are zero as there is no constraint in the axial direction. In real bearings such a constraint is provided by the axial flanges [11, 18]; however, this bearing is not designed to carry any axial preload.

Results for the misalignment in ball and roller bearings simulated by specifying a mean bearing angular displacement β_{ym} are shown in Figures 13 and 14 respectively. The dominant stiffness coefficients are the same as those seen for the radial preload case. For

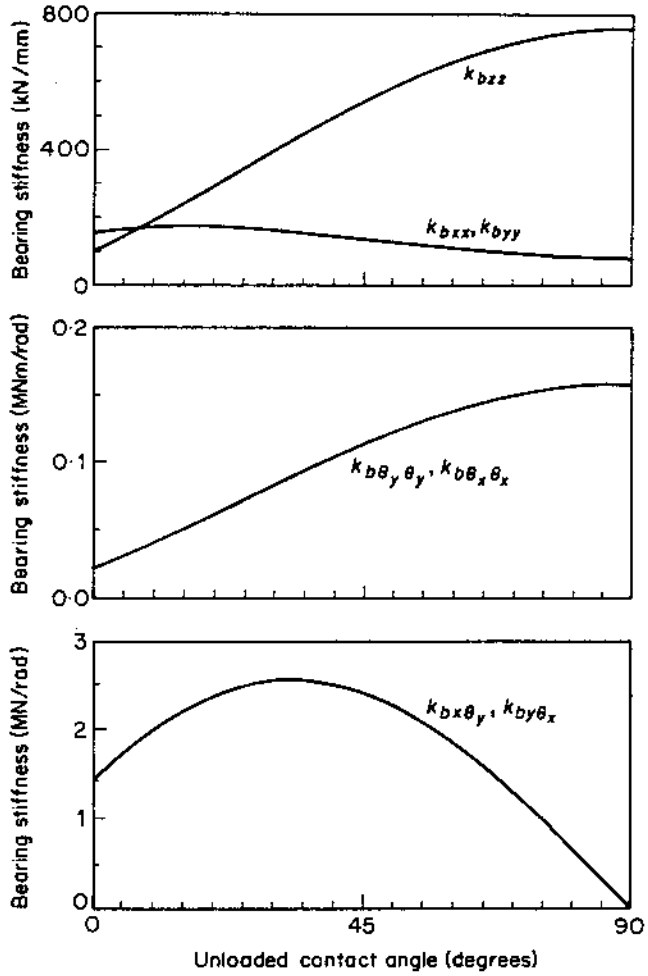

Figure 11. Dominant stiffness coefficients of ball bearing set A for $0° \leqslant \alpha_0 \leqslant 90°$ and given a constant mean axial bearing displacement $\delta_{zm} = 0{\cdot}025$ mm.

ball bearings, most of the stiffness coefficients remain constant for $0° \leqslant \alpha_0 \leqslant 90°$. On the other hand, the stiffness coefficients for roller bearing have trends similar to those found for the radial preload cases.

From the detailed parametric studies, it is concluded that the nature of $[K]_{bm}$ is dictated by the bearing type, α_0 and preloads. Also, the coupling coefficients are not negligible in most cases as assumed previously by many investigators.

9. CONCLUSIONS

Results of section 8, which show similar trends for some of the cases, imply that there may be a systematic approach to characterize the proposed bearing stiffness matrix $[K]_{bm}$. From the kinematic and geometrical considerations, it is always possible to impose any bearing displacement vector $\{q\}_{bm}$ which denotes relative rigid body motions between the inner and outer rings as long as the rolling element is still within the elastic deformation regime. On the other hand, an arbitrary application of $\{f\}_{bm}$ may not produce a singular displacement response from the bearing due to its kinematic and geometrical constraints. Hence, we have computed $[K]_{bm}$ and $\{f\}_{bm}$ by systematically varying $\{q\}_{bm}$. The results of all possible forms of $[K]_{bm}$ are listed in Tables 2 and 3 for ball and roller bearings

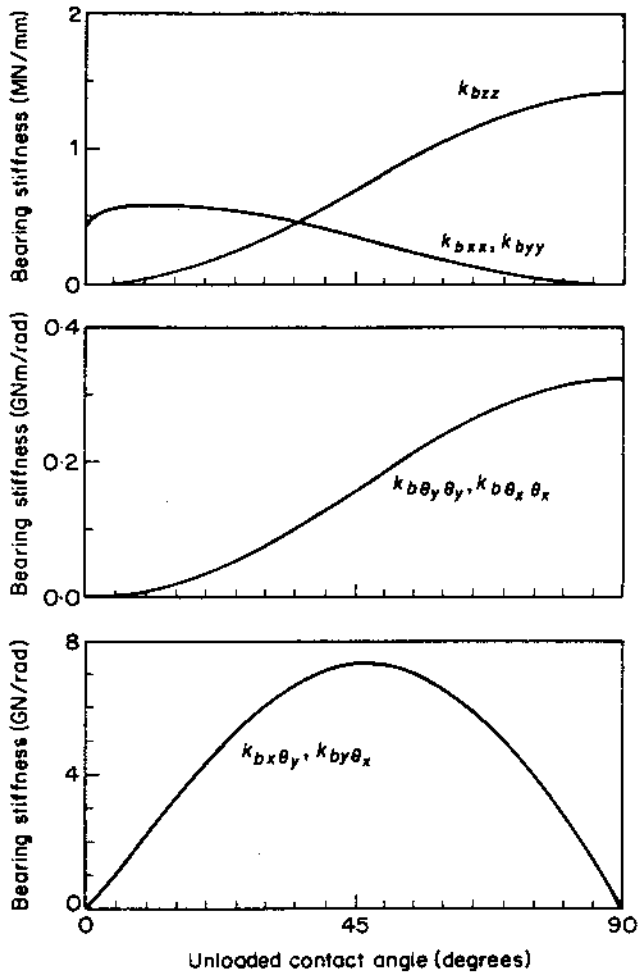

Figure 12. Dominant stiffness coefficients of roller bearing set B for $0° \leq \alpha_0 \leq 90°$ and given a constant mean axial bearing displacement $\delta_{zm} = 0{\cdot}025$ mm.

respectively. Also included here are the current bearing models which are based on the translational spring descriptions; these models do not show any coupling. Note that the exact values of the stiffness coefficients are not given as these depend on specific parameters; therefore only the dominant k_{bij} terms are listed for all possible bearing load configurations along with the corresponding $\{q\}_{bm}$ and α_0. Also, note that not all combinations of the bearing loads are possible, which complicates bearing stiffness calculations further, especially for the numerical method II. Tables 2 and 3 should provide some insight to the solution of the non-linear algebraic bearing load-deflection equations which requires *a priori* knowledge of the type of solution being sought as outlined earlier. In most practical problems, mean bearing loads are typically known. This knowledge can be combined with Tables 2 or 3 to formulate the non-linear load-deflection equations in the simplest form by deleting all of the zero displacement terms.

It is shown in Tables 2 and 3 that the coupling coefficients $k_{bx\theta_y}$, $k_{by\theta_x}$, $k_{bx\theta_x}$, $k_{bz\theta_y}$, $k_{b\theta_x\theta_x}$ and $k_{b\theta_y\theta_y}$ are found to be dominant in most of the ball bearing cases, and only in some of the roller bearing cases. This is essentially due to the curvature of the raceway in ball bearing which invariably causes the rolling element to orient itself such that $0° < \alpha_j < 90°$ which generates ball loads in the z direction as well. However, in the roller bearing case where $\alpha_j = \alpha_0$, the same phenomenon does not occur when $\alpha_0 = 0°$ or 90°, and the coupling coefficients are seen only when $\alpha_0 \neq 0°$ or 90°. In fact for the 0° and 90° unloaded contact angle cases, the stiffness coefficients associated with the x and y directions and those

TABLE 2

Comparison between the proposed and current ball bearing stiffness coefficients; $j = x, y$; $i = x, y$ but $i \neq j$

Mean bearing† loads	Mean bearing displacement			Dominant stiffness coefficients	
	$\alpha_0 \approx 0°$	$0° < \alpha_0 < 90°$	$\alpha_0 \approx 90°$	Current‡	Proposed§
F_{jm}	δ_{jm}	—	—	k_{jj}	$k_{xx}, k_{yy}, k_{zz}, k_{\theta_x\theta_x}, k_{\theta_y\theta_y}, k_{z\theta_i}$
F_{zm}	δ_{zm}	δ_{zm}	—	k_{jj}, k_{zz}	$k_{xx}, k_{yy}, k_{zz}, k_{\theta_x\theta_x}, k_{\theta_y\theta_y}, k_{x\theta_y}, k_{y\theta_x}$
F_{zm}	—	—	δ_{zm}	k_{zz}	$k_{xx}, k_{yy}, k_{zz}, k_{\theta_x\theta_x}, k_{\theta_i\theta_y}$
M_{jm}	β_{jm}	—	—	—	$k_{xx}, k_{yy}, k_{zz}, k_{\theta_x\theta_x}, k_{\theta_y\theta_y}, k_{iz}$
F_{zm}, M_{jm}	—	—	δ_{zm}, β_{jm}	k_{zz}	$k_{xx}, k_{yy}, k_{zz}, k_{\theta_x\theta_x}, k_{\theta_y\theta_y}, k_{z\theta_j}$
F_{xm}, F_{ym}	δ_{xm}, δ_{ym}	—	—	k_{jj}	$k_{xx}, k_{yy}, k_{zz}, k_{\theta_x\theta_x}, k_{\theta_y\theta_y}, k_{xy}, k_{\theta_x\theta_y}, k_{z\theta_x}, k_{z\theta_y}$
F_{jm}, M_{jm}	δ_{jm}, β_{jm}	—	—	k_{jj}	$k_{xx}, k_{yy}, k_{zz}, k_{\theta_x\theta_x}, k_{\theta_y\theta y}, k_{x\theta_x}, k_{y\theta_y}, k_{jz}, k_{z\theta_i}$
M_{xm}, M_{ym}	δ_{jm}, β_{jm}	—	—	—	$k_{xx}, k_{yy}, k_{zz}, k_{\theta_x\theta_x}, k_{\theta_u\theta_y}, k_{xy}, k_{xz}, k_{yz}, k_{\theta_x\theta_y}$
F_{jm}, F_{zm}, M_{im}	$\delta_{jm}, \delta_{zm}, \beta_{im}$	$\delta_{jm}, \delta_{zm}, \beta_{im}$	$\delta_{jm}, \delta_{zm}, \beta_{im}$	k_{jj}, k_{zz}	$k_{xx}, k_{yy}, k_{zz}, k_{\theta_x\theta_x}, k_{\theta_i\theta_y}, k_{x\theta_y}, k_{y\theta_x}, k_{jz}, k_{z\theta_i}$
F_{zm}, M_{xm}, M_{ym}	$\delta_{zm}, \beta_{xm}, \beta_{ym}$	$\delta_{zm}, \beta_{xm}, \beta_{ym}$	$\delta_{zm}, \beta_{xm}, \beta_{ym}$	k_{jj}, k_{zz}	$k_{xx}, k_{yy}, k_{zz}, k_{\theta_x\theta_x}, k_{\theta_y\theta_y}, k_{xy}, k_{\theta_x\theta_y}, k_{z\theta_x}, k_{z\theta_y}$
$\{f\}_m$	Combinations of $\{q\}_m$			k_{jj}, k_{zz}	All non-zero except θ_z terms

† Here the subscript b which implies bearing has been omitted for brevity.
‡ Ideal boundary condition models used to describe the bearing are not tabulated.
§ All terms associated with θ_z are zero because of the free rotation about the z axis.

TABLE 3

Comparison between the proposed and current roller bearing stiffness coefficients; $j = x, y$; $i = x, y$ but $i \neq j$

Mean bearing† loads	Mean bearing displacement			Dominant stiffness coefficients	
	$\alpha_0 \approx 0°$	$0° < \alpha_0 < 90°$	$\alpha_0 \approx 90°$	current‡	Proposed§
F_{jm}	δ_{jm}	—	—	k_{jj}	k_{bij}
F_{zm}	—	δ_{zm}	—	k_{jj}, k_{zz}	$k_{xx}, k_{yy}, k_{zz}, k_{\theta_x\theta_x}, k_{\theta_y\theta_y}, k_{x\theta_y}, k_{y\theta_x}$
F_{zm}	—	—	δ_{zm}	k_{zz}	$k_{zz}, k_{\theta_x\theta_x}, k_{\theta_y\theta_y}$
F_{zm}, M_{jm}	—	—	δ_{zm}, β_{jm}	k_{zz}	$k_{zz}, k_{\theta_x\theta_x}, k_{\theta_y\theta_y}, k_{z\theta_j}$
F_{xm}, F_{ym}	δ_{xm}, δ_{ym}	—	—	k_{jj}	k_{xx}, k_{yy}, k_{xy}
F_{jm}, F_{zm} M_{im}	—	δ_{jm}, δ_{zm} β_{im}	—	k_{jj}, k_{zz}	$k_{xx}, k_{yy}, k_{zz}, k_{\theta_x\theta_x}, k_{\theta_y\theta_y}, k_{x\theta_y}, k_{y\theta_x}, k_{jz}, k_{z\theta_i}$
F_{zm}, M_{xm}, M_{ym}	—	—	$\delta_{zm}, \beta_{xm}, \beta_{ym}$	k_{zz}	$k_{zz}, k_{\theta_x\theta_x}, k_{\theta_y\theta_y}, k_{\theta_x\theta_y}, k_{z\theta_x}, k_{z\theta_y}$
$\{f\}_m$	Combinations of $\{q\}_m$			k_{jj}, k_{zz}	All non-zero except θ_z terms

† Here the subscript b which implies bearing has been omitted for brevity.
‡ Ideal boundary condition models used to describe the bearing are not tabulated.
§ All terms associated with θ_z are zero because of the free rotation about the z axis.

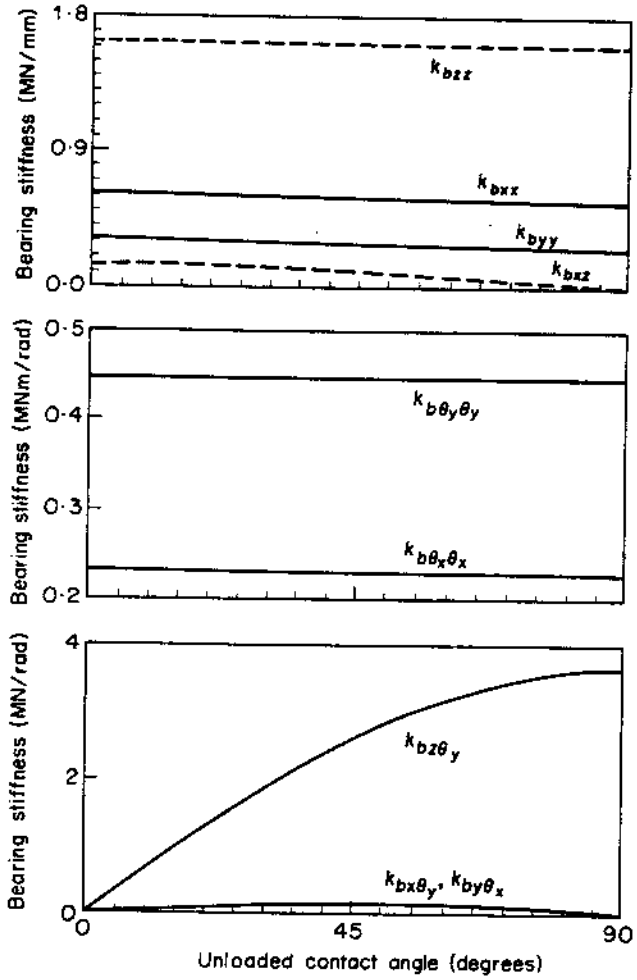

Figure 13. Dominant stiffness coefficients of ball bearing set A for $0° \leq \alpha_0 \leq 90°$ and given a constant misalignment $\beta_{ym} = 0{\cdot}015$ rad.

associated with the z, θ_x, and θ_y directions do not exist simultaneously; the former is dominant when $\alpha_0 = 0$ and the latter prevails when $\alpha_0 = 90°$. Another case of interest here is the case when bearing loads are complex, as given by the last row in Tables 2 and 3, where all of the bearing stiffness coefficients unrelated to the rotational degree of freedom θ_z exist. Solution for these cases may require a large number of iterations.

In summary, we have developed a comprehensive bearing stiffness matrix from the basic principles which includes all possible rigid-body degrees of freedom of a bearing system. This matrix has been validated partially using several analytical and experimental examples. Further validation of $[K]_{bm}$ is not possible as coupling coefficients are never measured [16, 17]. Nonetheless, our theory is general in nature and is applicable to even those configurations which may be different from the generic case shown in Figure 1. Further research is required to incorporate tribological issues [19, 20] in this formulation. However the proposed stiffness matrix in its present form, unlike the current models, is clearly capable of explaining the nature of vibration transmission through bearings—this is the subject of the companion paper, Part II [25], which also includes further comparisons between theory and experiment.

ACKNOWLEDGMENT

We wish to thank the NASA Lewis Research Center for supporting this research.

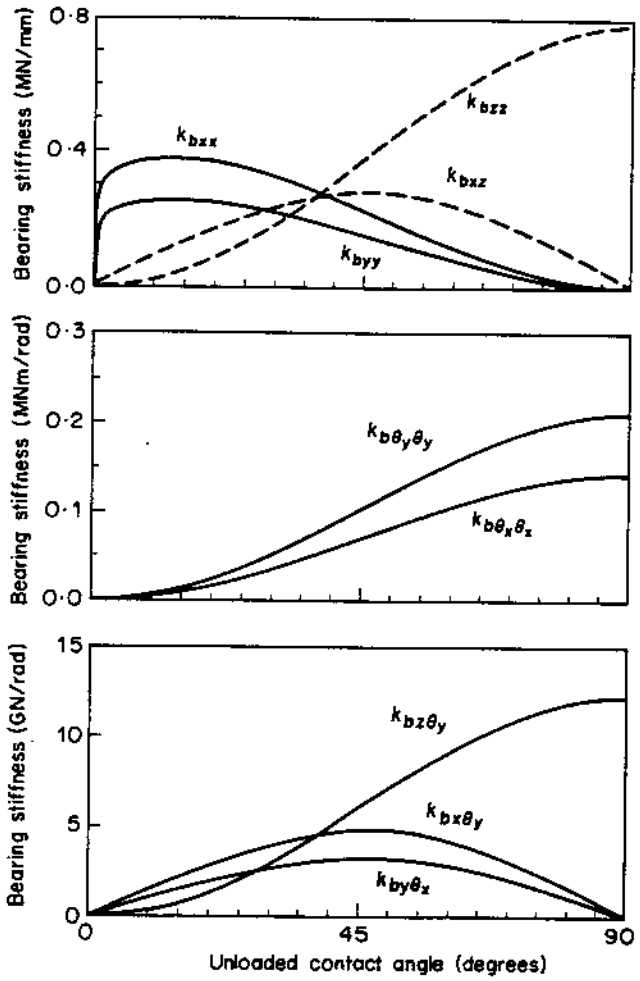

Figure 14. Dominant stiffness coefficients of roller bearing set B for $0° \leqslant \alpha_0 \leqslant 90°$ and given a constant misalignment $\beta_{ym} = 0{\cdot}015$ rad.

REFERENCES

1. H. N. OZGUVEN 1984 *Journal of Vibration, Acoustics, Stress, and Reliability in Design, Transactions of the American Society of Mechanical Engineers* **106**, 59–61. On the critical speed of continuous shaft-disk systems.
2. A. D. DIMAROGONAS and S. A. PAIPETIS 1983 *Analytical Methods in Rotor Dynamics.* London: Applied Science.
3. J. S. RAO 1983 *Rotor Dynamics.* New York: John Wiley.
4. E. S. ZORZI and H. D. NELSON 1977 *Journal of Engineering for Power, Transactions of the American Society of Mechanical Engineers* **99**(1), 71–77. Finite element simulation of rotor-bearing systems with internal damping.
5. E. P. GARGIULO 1980 *Machine Design* **52**, 107–110. A simple way to estimate bearing stiffness.
6. A. KAHRAMAN, H. N. OZGUVEN, D. R. HOUSER and J. J. ZAKRAJSEK 1989 *Proceedings of the International Power Transmission and Gearing Conference, Chicago,* 375–382. Dynamic analysis of geared rotors by finite elements.
7. K. ISHIDA, T. MATSUDA and M. FUKUI 1981 *Proceedings of the International Symposium on Gearing and Power Transmissions, Tokyo,* 13–18. Effect of gearbox on noise reduction of geared device.
8. A. M. MITCHELL, F. B. OSWALD and H. H. COE 1986 *NASA Technical Report* 2626. Testing of UH-60A helicopter transmission in NASA Lewis 2240kW(3000-hp) facility.
9. J. S. LIN 1989 *M.S. Thesis, The Ohio State University.* Experimental analysis of dynamic force transmissibility through bearings.
10. M. F. WHITE 1979 *Journal of Applied Mechanics* **46**, 677–684. Rolling element bearing vibration transfer characteristics: effect of stiffness.
11. T. A. HARRIS 1966 *Rolling Bearing Analysis.* New York: John Wiley.

12. A. PALMGREN 1959 *Ball and Roller Bearing Engineering.* Philadelphia: S. H. Burbank.
13. M. D. RAJAB 1982 *Ph.D. Dissertation, The Ohio State University.* Modeling of the transmissibility through rolling element bearing under radial and moment loads.
14. W. B. YOUNG 1988 *M.S. Thesis, The Ohio State University.* Dynamic modeling and experimental measurements of a gear shaft and housing system.
15. D. R. HOUSER, G. L. KINZEL, W. B. YOUNG and M. D. RAJAB 1989 *Proceedings of the Seventh International Modal Analysis Conference, Las Vegas,* 147–153. Force transmissibility through rolling contact bearings.
16. T. L. H. WALFORD and B. J. STONE 1980 *Journal of Mechanical Engineering Science* **22**(4), 175–181. The measurement of the radial stiffness of rolling element bearings under oscillation conditions.
17. J. KRAUS, J. J. BLECH and S. G. BRAUN 1987 *Journal of Vibration, Acoustics, Stress, and Reliability in Design, Transactions of the American Society of Mechanical Engineers* **109**, 235–240. *In situ* determination of rolling bearing stiffness and damping by modal analysis.
18. P. ESCHMANN, L., HASBARGEN and K. WEIGAND 1985 *Ball and Roller Bearings.* New York: John Wiley.
19. B. J. HAMROCK and W. J. ANDERSON 1983 *NASA Reference Publication* 1105. Rolling-element bearings.
20. P. K. GUPTA 1984 *Advanced Dynamics of Rolling Elements.* Berlin: Springer-Verlag.
21. A. B. JONES 1946 *New Departure Engineering Data, General Motors.* Analysis of stresses and deflections.
22. R. R. DAVIS 1988 *Proceedings of the Second International Symposium on Transport Phenomena, Dynamics and Design of Rotating Machinery, Honolulu,* 241–254. Incorporating general race and housing flexibility and deadband in rolling element bearing analysis.
23. W. H. PRESS, B. P. FLANNERY, S. A. TEUKOLSKY and W. T. VETTERLING 1986 *Numerical Recipes.* Cambridge: Cambridge University Press.
24. J. ORTEGA and W. RHEINBOLDT 1970 *Iterative Solution of Nonlinear Equations in Several Variables.* New York: Academic Press.
25. T. C. LIM and R. SINGH 1990 *Journal of Sound and Vibration* **139**(2), 201–225. Vibration transmission through rolling element bearings, part II: system studies.

APPENDIX: LIST OF SYMBOLS

A_0	unloaded distance between the inner and outer raceway groove curvatuve centers
A_j	loaded distance between the inner and outer raceway groove curvature centers
a_o, a_i	locations of the outer and inner raceway groove curvature centers
d_{bi}	inner raceway diameter of bearing
d_{bm}	bearing pitch diameter
d_{bo}	outer raceway diameter of bearing
F_{bim}	mean bearing force in the $i = x$, y or z direction
F_{im}	applied mean force on the shaft, $i = x$, y or z
$\{f\}_{bm}$	mean bearing load vector
$\{f\}_{sm}$	mean shaft load vector
G	bearing outer ring geometrical center
H_k	non-linear functions, $k = 1, 2, 3, \ldots, V$, given by equations (12a, b) and (13)
K_n	rolling element load-deflection stiffness constant
$[K]_{bm}$	proposed bearing stiffness matrix of dimension six
k_{bij}	bearing stiffness coefficient, $i, j = x, y, z, \theta_x, \theta_y, \theta_z$
$\hat{k}_{bij}$	estimated bearing stiffness coefficient, $i, j = x, y, z, \theta_x, \theta_y, \theta_z$
M_{bpm}	mean bearing moment about $p = x$ or y direction
n	rolling element load-deflection exponent
Q_j	resultant normal load on the jth rolling element
$\{q\}_b$	total bearing displacement vector
$\{q\}_{ba}$	alternating bearing displacement vector
$\{q\}_{bm}$	mean bearing displacement vector
$\{q\}_{sm}$	mean shaft displacement vector
r_j	pitch radius (roller) or radii of inner raceway groove curvature centers (ball)
r_L	bearing radial clearance
T_{im}	applied mean torque on the shaft, $i = x$, y or z

t	time
u_{im}	mean shaft translational displacement in the $i = x$, y or z direction
X	solution to the problem $H_k = 0$, $k = 1, 2, 3, \ldots, V$
Z	total number of rolling elements
z	number of loaded rolling elements
α_0	unloaded bearing contact angle
α_j	loaded jth rolling element contact angle
β_{pm}	mean bearing rotational displacement about the $p = x$ or y direction
ΔF_{brm}	incremental mean radial bearing force
$\Delta\delta_{rm}$	incremental mean radial bearing displacement
δ_{Bj}	resultant elastic deformation of the jth ball element
δ_{Rj}	resultant elastic deformation of the jth roller element
δ_{im}	mean bearing translational displacement in the $i = x$, y or z direction
δ_j	resultant elastic deformation of the jth rolling element
δX	error vector
$(\delta)_{rj}$	effective jth rolling element displacement in the radial direction
$(\delta)_{zj}$	effective jth rolling element displacement in the axial direction
θ_{im}	mean shaft angular displacement about the i-axis; $i = x, y, z$
Ω_z	mean rotational speed of the shaft
ψ_j	angular distance of jth rolling element from the x-axis
ψ_l	bearing load angle
$[\ ]^T$	transpose of a matrix or vector